Geophysical Research Letters

16 JANUARY 2007
Volume 34 Number 1
American Geophysical Union

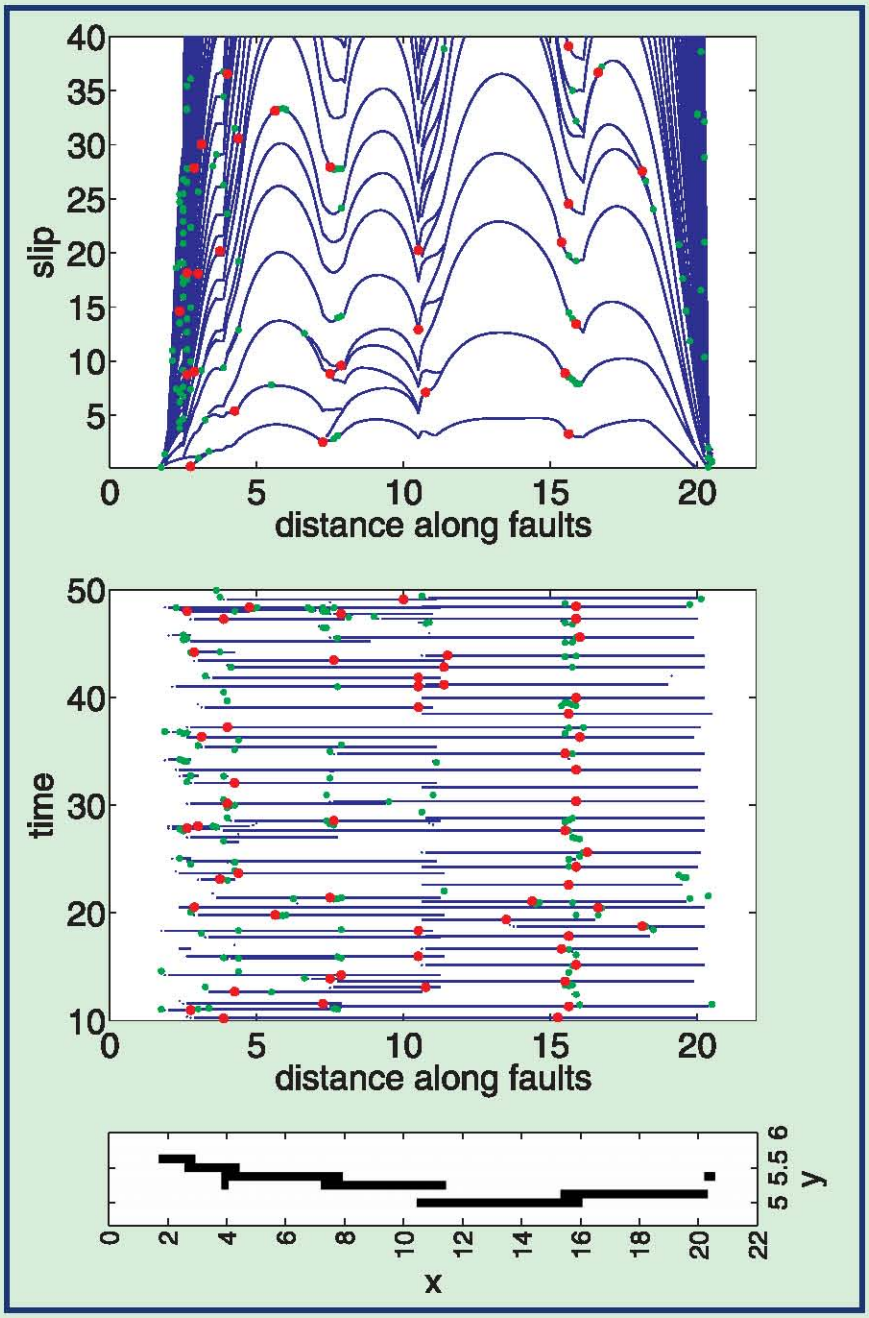

Toward a more objective determination of seismic hazards • Andaman Islands deformation associated with the 2004 Sumatra-Andaman earthquake • Decomposing methane gas hydrates on the Arctic Shelf? • Typhoon-induced solitary waves off the east coast of Korea

GEOPHYSICAL RESEARCH LETTERS, VOL. 34, L01307, doi:10.1029/2006GL027980, 2007

Probabilities for jumping fault segment stepovers

Bruce E. Shaw[1] and James H. Dieterich[2]

Received 27 August 2006; revised 2 November 2006; accepted 30 November 2006; published 11 January 2007.

[1] Seismic hazard analysis relies heavily on the segmentation of faults. The ability of ruptures to break multiple segments has a big impact on estimated hazard. Current practice for estimating multiple segment breakage relies on panels of experts voting on their opinions for each case. Here, we explore the probability of elastodynamic ruptures jumping segment stepovers in numerical simulations of segmented fault systems. We find a simple functional form for the probability of jumping a segment stepover as a function of stepover distance: an exponential falloff with distance. We suggest this simple parameterization of jumping probabilities, combined with sparse observational data to fix the lengthscale parameter, as a new approach to estimating multisegment earthquake hazard. **Citation:** Shaw, B. E., and J. H. Dieterich (2007), Probabilities for jumping fault segment stepovers, *Geophys. Res. Lett.*, *34*, L01307, doi:10.1029/2006GL027980.

1. Introduction

[2] Fault segmentation has played a central role in traditional seismic hazard analysis, with ruptures assumed to break all of a segment, and sometimes cascade across segments to break one or a few segments. These assumptions impact hazard in a number of ways. Since the largest ruptures dominate the moment sum, the resulting distribution of them sets not only the rate of large events, but the rate of more numerous moderate events as well, both of which can impact the local hazard. Further, the boundaries of segments play an additional role in creating hazard hotspots, where events from multiple nearby segments increase the rate of occurrence of strong shaking. Yet the relationship between earthquakes and segmentation appears much more complex than these standard treatments have accounted for. The 1992 M7.1 Landers earthquake jumped two segment stepovers before dying in the middle of another segment. The 2002 M7.9 Denali earthquake began on a thrust fault, transferred to a strike-slip fault, then branched onto a different fault as the rupture died on the main fault. Clearly, a better understanding of how fault segment geometry impacts large earthquake ruptures is needed.

[3] *Harris et al.* [1991] and *Harris and Day* [1999] initiated theoretical studies of the ability of ruptures to jump segment stepovers, finding it difficult for ruptures to jump distances larger than 5 km for the conditions they considered. A number of groups have further explored the ability of individual ruptures to jump a variety of stepover configurations and faulting mechanisms [*Kase and Kuge*, 1998; *Anderson et al.*, 2003; *Oglesby*, 2005; *Aochi et al.*, 2005].

[4] For seismic hazard analysis, however, we need not just a statement of what is possible, but how likely it is: we need probabilistic statements about segments breaking together. In the absence of a better way to do it, this has meant in practice that an expert panel has voted on what their opinion is about the likelihood of various segments rupturing separately or together [*Working Group on California Earthquake Probabilities*, 2002]. A more objective basis for this would clearly be useful.

[5] In this paper, we examine the question of the probability of jumping segment stepovers, using a model which both generates a complex segmented fault geometry and generates long sequences of elastodynamic ruptures on that complex fault geometry. The model is simplified in a number of ways, being two dimensional, and considering only the geometrical irregularities of segment stepovers, among other simplifications. Our results, however, appear very simple as well, and thus we believe useful to the real problem at hand. In particular, we find an exponential decrease in the probability of jumping a segment stepover as the stepover distance increases. This scale length for the jumping probability falloff depends weakly on a number of different physical parameters in the model, but the functional form appears quite robust. Thus, we can reduce the parameterization of the real system to the value of this scale length.

2. Model

[6] The model makes a number of simplifications, but by making these simplifications allows for the study of long sequences of elastodynamic events on a geometrically complex fault system. The model is two dimensional, collapsing the depth dimension so all the degrees of freedom occur in map view. The model is scalar, so normal stress changes are effectively neglected in the problem. Faults are restricted to break in only one direction, limiting the geometrical irregularities to segment ends and stepovers. Nevertheless, remarkably rich fault system geometries and sequences of events develop in this model.

[7] The fault geometry is not specified. Rather, a physics is specified, out of which a fault system grows. In particular, we consider a geological slip weakening, so the more a fault slips the weaker it gets. This weakening localizes slip onto faults. Beginning from an initial condition of an unbroken plate with small uncorrelated random strength heterogeneities, a fault system develops as the system is loaded, with slip localizing onto faults with a wide range of segment lengths [*Spyropoulos et al.*, 2002]. Because the fault system which develops has organized itself, stress singularities do

[1]Lamont-Doherty Earth Observatory, Columbia University, Palisades, New York, USA.
[2]Department of Earth Science, University of California, Riverside, California, USA.

0094-8276/07/2006GL027980$05.00

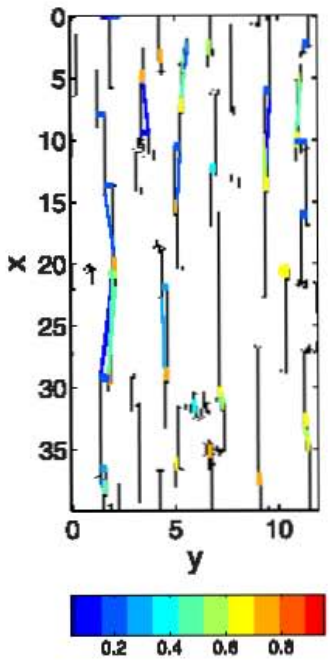

Figure 1. Map view of fault system, and segment jumping probabilities. Black lines show faults which have slipped. Colored lines indicate jumping probabilities. Colored lines connect segments which have both slipped during the same large event. Width of colored lines are inversely proportional to closest distance separating segments. Color of line indicates probability of both segments rupturing when one of them ruptures. Note longer distances (longer thinner lines) tend to have lower jumping probabilities (bluer colors).

not grow despite the nonuniform fault geometry; if stresses build up, they simply grow a new fault. Distributions of lengths of fault segments in the strain regimes we examine here are power-law-like with exponential cutoffs at the largest segments [*Shaw*, 2004a]. Typical domain sizes contain a hundred long segments– segments greater than the length scale unity of the seismogenic crust depth– with many more smaller fault segments as well.

[8] Once a nicely localized fault system has developed, we examine long sequences of elastodynamic events on this system [*Shaw*, 2004a]. These timescales are much shorter than the millions of year geological timescales over which the fault systems develop, but much longer than individual rupture events or a large event cycle, being tens of large event cycles corresponding to many thousands of years. These long sequences of events are essential to the problem, as they allow the stress fields to organize as well to accommodate the physics operating on the fast dynamic rupture timescale. This is a key point: the initial stress before a rupture comes through has a huge impact on the ability of a rupture to jump a segment stepover, so the distribution of initial stresses is a fundamental ingredient to determining jumping probabilities. And only by examining long sequences of events can we obtain the appropriate distribution of initial stresses.

[9] The equations describing the model have been presented elsewhere [*Shaw*, 2004a, 2004b, 2006]. The model shows a number of interesting behaviors relevant to hazard estimates. In the work by *Shaw* [2004a] the distribution of sizes of events was studied; a modified segmentation hypothesis was found, with segments most commonly breaking as a unit, but also sometimes breaking only party in power-law small events and sometimes cascading into multiple segment ruptures. In the work by *Shaw* [2004b] the coefficient of variation of large event ruptures was examined, with both time variation and slip variation studied, and found to be nonuniform in space. We found higher variation at segment ends, and found that longer segments have lower variation. In the work by *Shaw* [2006] the initiation, propagation, and termination of ruptures was studied and found to be associated with segment ends and stepovers. Shaking hazard was measured directly in the models, producing hazard maps from a physics without need for additional parameterizations. Here we step back from that full capability, to examine aspects of the underlying ruptures which could be used for parameterizations to construct hazard maps. In particular, we examine the question of ruptures jumping segment stepovers.

3. Results

[10] We measure jump probabilities the following way. First, every point in space which has slipped is assigned to a fault segment. Because we are operating on a lattice and only allow faults to break in one direction, perpendicular to the loading y direction, we end up with an array of parallel faults of varying lengths in the x direction. The segments are thus easily defined as a contiguous length of fault in the x direction all at the same value of y. All lengths in the problem are scaled to the seismogenic fault down-dip width, so a length of unity corresponds to roughly 15 km in a vertical strike-slip fault. For typical domain sizes we compute this gives some hundreds of fault segments. This number n of segments is small enough then to keep track of the cross-correlation matrix of size n^2, which keeps track of whether an event which ruptured on segment j also ruptures on segment j'. That is, for every event in the long catalogue, we measure the segments it broke, increment a counter N for each segment it broke, and a counter for the cross correlation of each pair of segments which also broke. The probability of jumping the segments is then the cross-correlation counters divided by the segment counters:

$$p(j,j') = \frac{N(j,j') + N(j',j)}{N(j) + N(j')} \tag{1}$$

In order to measure only jumps which we care about–large events which slip a significant amount–we set a threshold on the minimum slip level needed somewhere on a segment in an event to have that segment count as having slipped. We calculate distance between segments as the closest euclidean distance between two segments.

[11] Figure 1 shows the result of this effort in map view. The faults are colored black. The jumping probabilities are color coded with red colors being higher probability of jumping and blue colors being lower probability of jumping. The thickness of the lines scales inversely with the closest distance between segments, and connects the closest

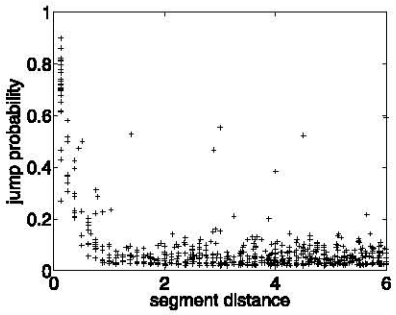

Figure 2. Scatter plot of jump probabilities as a function of segment separation distance. Each point corresponds to a segment pair. Only segment pairs which had at least one jump are shown.

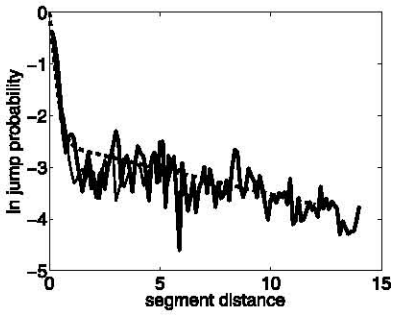

Figure 4. Functional form of mean jumping probability. Log jump probability versus linear distance. Straight line indicates exponential falloff. Functional form fit with two exponentials, one fast falloff at short distance, and one slower falloff at large distance. Dashed line shows equation (2) fit with parameters $r_0 = .2$, $\epsilon = .08$, $r_1 = 10$. The two different thickness lines show two different domain sizes; they are hard to distinguish, and show the lack of dependence on domain size.

points between the two segments. In this plot, we show only whether two segments participated in the same event, not whether other segments also participated. Note, however, that intermediate connecting segments can also participate in a rupture, and longer distance connections appearing in this map view plot most often occur through the linking segments. Later, we will make a cut to the data to account for the linking segments. Only segment pairs which had a jumping event are shown. There are periodic boundary conditions in the model, but for ease of visualization we have left off the lines which wrap around the boundaries. One clear thing to notice in Figure 1 is that the closet segments–the thicker lines–tend to have redder colors. We will explore this effect more quantitatively in the plots which follow, where we neglect spatial locations and just look at jumping probabilities between segments as a function of segment distance.

[12] Figure 2 shows a scatter plot of jump probabilities as a function of jump distance. Only segment pairs for which at least one jump has been made are plotted, so no zero probability points are shown. Not too surprisingly, we see a clear trend of much higher probabilities at short distances falling off to lower probabilities at greater distances. At the same time, we see a few relatively high probabilities at somewhat large distances. These points arise, however, from intervening linking faults which allow the ruptures to jump a relatively small distance, propagating along the linking fault, before jumping a second small distance. These cases show up in Figure 1 as long distance links at low angles relative to the fault. A simple cut to the data, requiring the fault perpendicular y distance to be at least as large as the fault parallel x jump distance gets rid of these anomalies. This is shown in Figure 3, along with the zero probability points which were excluded in Figure 2, which then allows for the plotting of a mean probability, shown with the solid line. This mean probability forms the basis of the rest of our plots which follow, all of which use the data cut for fault perpendicular jump at least as large as fault parallel jump. One interesting aspect of these distributions of probabilities at a given distance are the existence of zeros of jumping cases even at short distances. We focus in this paper on the mean behaviors, but the question of whether there are particular geometries that remain true barriers to jumping even over extremely long sequences of events is an interesting question for further study.

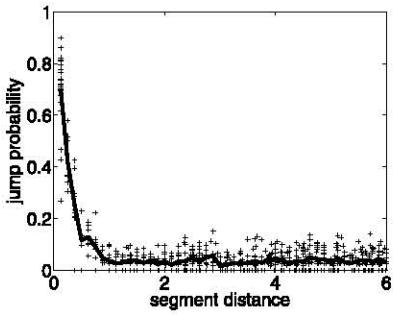

Figure 3. Scatter plot of jump probabilities as a function of segment separation distance. Only segments with fault perpendicular separation distance at least as large as fault parallel separation distance are shown. Zero probability pairs are included as well, allowing for mean jump probability to be calculated, shown with solid line.

[13] Plotting the log of the jump probability versus the linear distance of separation, Figure 4 shows a key result: the jump probability is seen to fall off exponentially at short distances, followed by a slower exponential falloff at larger distances. Specifically, we find

$$p(r) = e^{-r/r_0} + \epsilon\left(e^{-r/r_1} - e^{-r/r_0}\right) \qquad (2)$$

is a good fit to the probability p distribution dependence on distance r, with $\epsilon \ll 1$ and $r_0 < r_1$. This provides a one parameter fit r_0 at short distances, a fitting which is likely to be sufficient for hazard purposes. A further fit of a constant level ϵ at intermediate distances $r_0 < r < r_1$, and r_1 at large distances $r_1 < r$ can be made as well. Note that the probability distribution has the important continuity property that at zero distance the jump probability is unity.

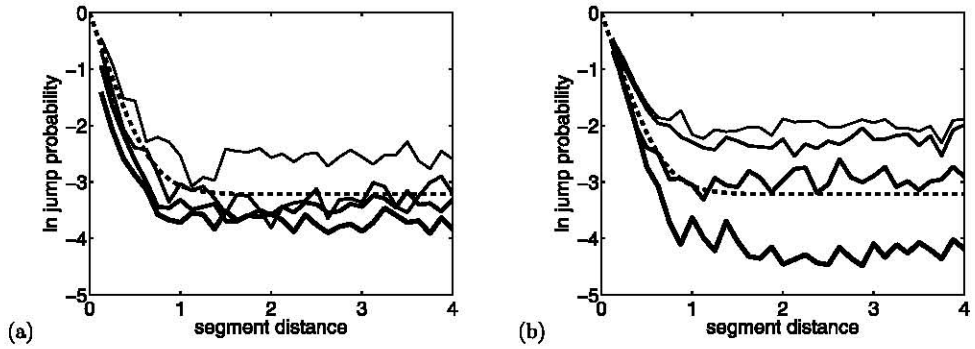

Figure 5. Average jump probabilities with changing dissipation. (a) Fault dissipation. (b) Bulk dissipation. Dashed line fit with equation (2). Increasing line thickness corresponds to increasing dissipation. (Dissipation parameters: For Figure 5a, geological slip weakening rate $\beta = .4, .3, .1$. For Figure 5b, bulk dissipation inverse length $\eta = .0125, .05, .2, .8$. See *Shaw* [2006] for discussion of dissipation parameters.) Dashed line shows equation (2) fit with parameters $r_0 = .2$, $\epsilon = .04$ and r_1 large enough to be irrelevant.

[14] We next explore how these fitting parameters depend on different source physics. We need large domains to explore very large r, which is quite expensive numerically, so we will focus our attention on small and intermediate values of r where r_0 and ϵ can be easily studied. Figure 5 shows a plot where we change the amount of dissipation in the problem. In Figure 5a, we change the dissipation on the fault, changing the degree of geological slip weakening in the problem. In Figure 5b, we change the dissipation in the bulk, changing the degree to which waves are damped in the bulk. In both plots thicker lines are higher dissipation. In both plots similar effects can be seen: higher dissipation leads to a somewhat faster falloff with distance–smaller r_0– and a lower intermediate amplitude ϵ.

[15] Figure 6 shows a plot where we examine different geological eras in the fault evolution history, with earlier geological eras having more active smaller faults and later eras a more localized system with longer segments and fewer active small faults. The results are little changed, showing that the detailed fault geometry matters much less than the dissipation mechanisms.

4. Conclusion

[16] We have found a functional form for jump probabilities which appears robustly across a wide range of parameters in our models. This form has a number of desirable features for parameterizing this important feature of dynamic ruptures: continuity at zero jump distance, zero probability at large distance, continuous decrease in between, and simplicity. At its most basic level, it proposes a single fitting parameter, a lengthscale for an exponential falloff in probability of jumping a given distance. A second parameter can be fit at intermediated distances, a constant probability, and a third parameter can be fit at large distances, a slower exponential falloff. In practice, we anticipate the one parameter fit of the exponential falloff lengthscale r_0 being sufficient for hazard estimates. While our numerical calculations do not fix this value (although they do typically find values which appear quite reasonable– e.g. Figure 4 has $r_0 \sim W/5 \sim 3$ km, using $W = 15$ km for strike-slip faults), they do provide a framework for looking at the limited new observational data just now becoming available [*Wesnousky*, 2006]. Combining this theoretical work with the limited but crucial observational data [*Wesnousky*, 2006], we propose a first order model for use in hazard maps of a probability for jumping

$$p(r) = e^{-r/r_0} \tag{3}$$

with the value of r_0 to be fit by the limited data. It might be anticipated that r_0 could differ for different faulting mechanisms, thrust versus normal or strike-slip, or different types of stepovers, extensional versus compressional. More sophisticated models dealing with the full tensor dynamics including normal stress effects should give some further insight into these questions, work we are currently pursuing. Furthermore, other types of geometrical irregularities need to also be considered, such as bends in faults. These generalized geometrical irregularities are for now beyond the capability of our current models, but are not beyond the capacity of generalizations of our approach.

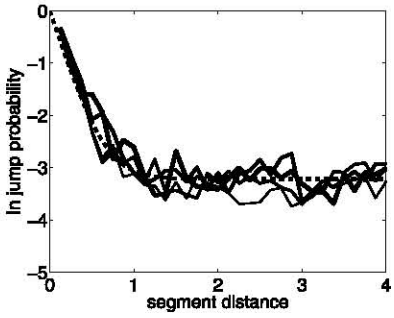

Figure 6. Average jump probabilities with changing stages of geological strain. Increasing line thickness corresponds to increasing age. Note little geological age dependence. Dashed line shows equation (2) with $r_0 = .2$, $\epsilon = .04$ and r_1 large enough to be irrelevant.

[17] **Acknowledgments.** We thank Ned Field and Mike Vredevoogd for discussions which helped motivate this work. We thank Martin Mai for comments on the manuscript. Part of this work was done while the authors were at the KITP in Santa Barbara. This work is partially supported by NSF EAR03-37226 and by the Southern California Earthquake Center (SCEC). This research was supported in part by the National Science Foundation under grant PHY99-0794.

References

Anderson, G., B. Aagaard, and K. Hudnut (2003), Fault interactions and large complex earthquakes in the Los Angeles area, *Science, 302*, 5652.

Aochi, H., O. Scotti, and C. Berge-Thierry (2005), Dynamic transfer of rupture across differently oriented segments in a complex 3-D fault system, *Geophys. Res. Lett., 32*, L21304, doi:10.1029/2005GL024158.

Harris, R. A., and S. M. Day (1999), Dynamic 3D simulations of earthquake on en echelon fault, *Geophys. Res. Lett., 26*, 2089.

Harris, R. A., R. J. Archuletta, and S. M. Day (1991), Fault steps and the dynamic rupture process: 2-D numerical simulations of a spontaneously propagating shear fracture, *Geophys. Res. Lett., 18*, 893.

Kase, Y., and K. Kuge (1998), Numerical simulation of spontaneous rupture processes on two non-coplanar faults: The effect of geometry on fault interaction, *Geophys. J. Int., 135*, 911.

Oglesby, D. D. (2005), The dynamics of strike-slip step-overs with linking dip-slip faults, *Bull. Seismol. Soc. Am., 95*, 1604.

Shaw, B. E. (2004a), Self-organizing fault systems and self-organizing elastodynamic events on them: Geometry and the distribution of sizes of events, *Geophys. Res. Lett.*, L17603, doi:10.1029/2004GL019726.

Shaw, B. E. (2004b), Variation of large elastodynamic earthquakes on complex fault systems, *Geophys. Res. Lett.*, L18609, doi:10.1029/2004GL019943.

Shaw, B. E. (2006), Initiation propagation and termination of elastodynamic ruptures associated with segmentation of faults and shaking hazard, *J. Geophys. Res., 111*, B08302, doi:10.1029/2005JB004093.

Spyropoulos, C., C. H. Scholz, and B. E. Shaw (2002), Transition regimes for growing crack populations, *Phys. Rev. E, 65*, 056105.

Wesnousky, S. G. (2006), Predicting the endpoints of earthquake ruptures, *Nature, 444*, 356, doi:10.1038/nature0527.

Working Group on California Earthquake Probabilities (2002), Earthquake probabilities in the San Francisco Bay Region: 2002 to 2031, *U.S. Geol. Surv. Circ., 1189*.

J. Dieterich, Department of Earth Science, University of California, Riverside, CA 92521, USA. (james.dieterich@ucr.edu)

B. Shaw, Lamont-Doherty Earth Observatory, 61 Rte 9W, Palisades, NY 10964, USA. (shaw@ldeo.columbia.edu)